Evaluation of TLS and PMLS Sensors for Cultural Heritage Documentation and HBIM Modelling: The Case Study of San Giacomo Church in Como, Italy

Manuel Garramone [1*], Luigi Barazzetti [1], Marco Scaioni [1]

[1] Dept. of Architecture, Built Environment and Construction Engineering, Politecnico di Milano, via Ponzio 31, 20133 Milano, Italy
(manuel.garramone, luigi.barazzetti, marco.scaioni)@polimi.it

Keywords: Building Information Modelling (BIM), Cultural Heritage, HBIM, Scan-to-BIM, Simultaneous Localisation and Mapping (SLAM), Terrestrial Laser Scanning (TLS).

Abstract

Static Terrestrial Laser Scanning (TLS) and SLAM-based Portable Mobile Laser Scanning (PMLS) are increasingly adopted in Cultural Heritage (CH) documentation, but their suitability for Historic/Heritage Building Information Modelling (HBIM) depends on both data quality and acquisition conditions. This paper compares a 2022 TLS survey and a 2025 handheld PMLS survey of San Giacomo Church (Como, Italy) to assess whether the latter can reliably support HBIM-oriented documentation. The methodology combines dataset-level comparison and ROI-based analysis on four stable architectural elements: apsis, pillar, timber roof truss, and central dome. Three complementary metrics were used: a local density proxy, a scale-dependent coverage ratio, and M3C2 distance statistics for geometric agreement. Results show that PMLS is consistently less dense than TLS but remains effective for 1:100 scale documentation and, in several cases, also for 1:50. Statistics on M3C2 distance remain generally within centimetric ranges, indicating good local agreement where surfaces are effectively observed. The study demonstrates that sensor suitability not only depends on the geometric complexity but also on sensor-to-surface distance, visibility, and acquisition geometry, supporting hybrid TLS–PMLS workflows for CH HBIM.

1. Introduction

Static Terrestrial Laser Scanning (TLS) and Portable Mobile Laser Scanning (PMLS) based on SLAM technology (Scaioni et al., 2025) are two prominent solutions for 3D documentation in Cultural Heritage (CH) and Building Information Modelling (BIM). Both can be used for data acquisition (together with SfM photogrammetry from ground and drones, especially in large outdoor scenes or tall buildings – see Autelitano et al., 2023), but they vary in terms of accuracy, point cloud density, and efficiency (Warchoł et al., 2023). TLS can be considered as the state-of-the-art consolidated technique for 3D modelling of architectural heritage, while PMLS is emerging as a potential alternative/integration in some cases. In addition, the quick impressive development of mobile 3D ranging sensors allows to foresee a future high impact of PMLS for CH documentation, unlike it happened in the past with other type of sensors (e.g., solid cameras – see Altuntas et al., 2016).

This study compares TLS and PMLS for documenting San Giacomo Church in Como, Italy. The Romanesque church had previously been surveyed in 2022 with TLS for restoration and Historic/Heritage BIM (HBIM) creation purposes (Garramone et al., 2023). Building on that reference dataset, the present work investigates whether a SLAM-based handheld PMLS survey can provide a reliable and operationally efficient alternative or complement for HBIM-oriented documentation of CH buildings. In this study, the TLS dataset is used as the geometric benchmark for evaluating PMLS performance. The comparison is articulated around three complementary aspects: local point-cloud density, scale-dependent usable completeness, and geometric agreement with respect to the TLS reference. Survey accuracy is a first point of comparison: TLS is widely recognised for its high precision, enabled by static acquisition, controlled registration, and robust georeferencing procedures, which help preserve metric consistency even in complex environments (Liu et al., 2023) . By contrast, PMLS systems generally provide lower precision, typically at centimetric level, depending on the sensor, trajectory, and environmental conditions (Rashdi et al., 2024). However, this difference in nominal accuracy does not, by itself, determine whether the data are suitable for HBIM: the intended representation scale, the type of architectural element, and the acquisition geometry must also be considered (Del Duca & Machado, 2023).

Point-cloud density represents a second key aspect. TLS produces dense and detailed point clouds, often well suited to the reconstruction of complex architectural features (Oreni et al., 2025). PMLS systems instead generate less dense and more variable datasets, influenced by operator movement, sensor-to-surface distance, and local visibility conditions. Nevertheless, such datasets may still be adequate for modelling general geometries and for rapid documentation tasks, especially when detailed acquisition is not required throughout the whole building.

Efficiency is the third major difference. TLS acquisition is time-intensive, requiring station planning, tripod positioning, scan registration, and often multiple acquisitions to reduce occlusions, and this is particularly demanding in CH contexts (Chen et al., 2026). By contrast, PMLS requires minimal setup and allows fast walk-through acquisition, significantly reducing field time while still covering large portions of the building (Bae et al., 2025; Vassena, 2025). This makes PMLS especially attractive where access is limited, survey time is constrained, or rapid documentation is needed before or during restoration activities.

Beyond raw survey performance, the study addresses the implications of these differences for HBIM workflows. In HBIM applications, the quality of the source survey affects both the achievable Level of Detail (LoD, the granularity of geometric representation), and the Level of Accuracy (LoA, the degree to which the model reproduces measured geometry) , see Panayiotou & Kontovourkis (2024). TLS is generally more suitable when high detail and strict geometric control are required, while PMLS is potentially effective for rapid as-built surveys, preliminary documentation, or operational contexts where a lower level of geometric refinement is acceptable (Previtali et al., 2026).

Since the TLS and PMLS surveys were acquired in different years, this analysis focuses on selected stable Regions of Interest (ROIs), that were not visibly modified between the two acquisition campaigns. Within these ROIs, three metrics are used: (1) a local density proxy based on neighbourhood statistics, (2) a scale-dependent coverage ratio derived from TLS-to-PMLS cloud-to-cloud distances, and (3) M3C2 distance statistics describing local geometric agreement. This framework allows the comparison to be directly linked to HBIM representation needs at different scales.

San Giacomo Church provides a meaningful test case because of its architectural complexity and the presence of elements observed under very different survey geometries.

The main contribution of the paper is therefore twofold: (i) it proposes a structured ROI-based comparison framework for evaluating TLS and PMLS in HBIM-oriented documentation; (ii) it derives a decision matrix for selecting TLS, PMLS, or hybrid acquisition strategies according to element type, required representation scale, and acquisition conditions.

2. Case Study

San Giacomo is a Romanesque church in Como (Italy), founded in the 11th Century (see Fig. 1). From the Middle Ages until the 16th Century, it was part of the Cathedral complex and played a key role in the town's political life. Over time, the church underwent major transformations: until 1580 it had a much longer nave than today and helped close off the public square towards the Cathedral. Later, as the surrounding urban fabric densified and the church's prominence declined, a severe state of decay led to the demolition of part of the building in the late 16th Century. A new façade was then constructed in 1585 to close the truncated nave, and the remaining medieval structure was progressively reworked through Baroque transformations (Catalano, 2004).

Figure 1. - San Giacomo Church, Como (Italy).

The present study is framed within the ongoing conservation and restoration activities that began in 2022 (Della Torre & Rajabi, 2022). The broader project aims to restore the church and integrate it within the new Como Cathedral Museum, supporting a "cultural system" that enhances the heritage value of the site and requires interdisciplinary collaboration (e.g., historians, restorers, architects, archaeologists, engineers). Previous works stressed that documentation, geometric survey, archaeological investigation and diagnostic activities represent the first step toward understanding the building's transformations over centuries and its current conservation state, and toward planning and managing restoration works and future maintenance (Garramone et al., 2023).

In this context, HBIM is conceived as an operational tool rather than a purely geometric model: a continuously updatable digital environment to manage the heterogeneous information produced during restoration works (including both geometric and non-geometric data), and to support multiple uses such as planning restoration actions, coordinating on-site activities, supporting safety issues, and enabling future developments (e.g., the installation of monitoring systems for bearing elements).

2.1 Survey datasets overview

This study relies on two 3D survey datasets of San Giacomo Church acquired with different strategies and at different times. Table 1 reports the main characteristics of the adopted sensors and collected datasets.

Table 1. - TLS and PMLS survey datasets characteristics.

	TLS	SLAM
Date	2022	2025
Sensor / platform	FARO Focus HDR130 + FARO Focus S70	Stonex X70 GO
Acquisition mode	Static TLS (multi-station)	Handheld SLAM walk-through
Surveyed areas used in this study	Church dataset + roof dataset from UAV photogrammetry	Church dataset
No. of scans / sessions	>300 scans	1 session
Field effort	About 6 working days with two operators operating two scanners	Few minutes for calibration + about 2 hours acquisition; operators only
Output	6 registered TLS point clouds (~ 48.2 GB) + 1 roof point cloud (not considered in this study)	1 coloured (~ 4 GB) + 1 optimised (~ 5.5 GB) point clouds
No. of points	2,051,130,272 points	122,491,585 points (coloured); 167,418,631 points (optimised)

A TLS campaign, in 2022, produced a point cloud that is treated as the geometric benchmark, and it also supported the development of an HBIM model in Autodesk Revit®.

A second dataset was collected in 2025 using a portable, SLAM-based system, aimed at achieving rapid coverage of the church spaces.

Both point clouds (see Fig. 2) are compared at two complementary levels: (i) a dataset-level comparison provides an overall assessment of global geometric discrepancies; (ii) an element-oriented analysis is conducted on selected ROIs representing stable architectural components, to reduce the influence of temporal changes between both acquisitions and to relate geometric performance to HBIM modelling needs. The outcomes are then used to derive practical guidelines and a decision matrix linking sensor choice (TLS, PMLS, or hybrid) to the element type and the expected LoD/LoA requirements in scan-to-HBIM workflows.

After the survey, a metrological framework was established through a topographic control network measured with a Leica TS30 theodolite and supported by GNSS observations (Emlid Reach RS2, using the regional CORS infrastructure). The overall reference system was reported as ETRF2000-RDN/UTM zone 32N.

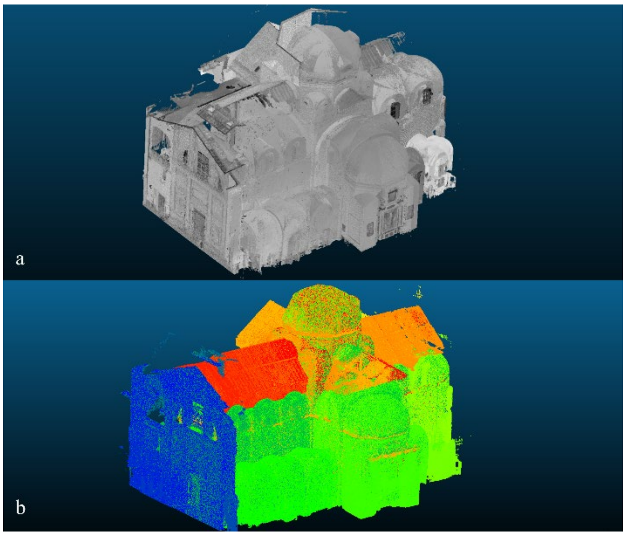

Figure 2. - Point cloud of the San Giacomo church from (a) the Terrestrial Laser Scanning (TLS) and (b) the Portable Mobile Laser Scanning (PMLS) survey (the colour distribution – blue-green-yellow-red – illustrates the operator’s trajectory and the temporal progression of the scanning process).

The accuracy indicates millimetric performance for the local control network (on the order of a few millimetres), millimetric scan registration residuals, and centimetric-level uncertainty for the GNSS-based georeferencing component, which is consistent with VRS/GNSS constraints in dense urban contexts. This step is fundamental because all distance-based metrics adopted in the study assume that the observed geometric discrepancies are primarily related to the sensor behaviour, acquisition geometry, or local incompleteness, rather than to residual rigid misalignment.

In order to ensure computational feasibility and to support a transparent interpretation of the results, both datasets were first characterised in terms of point-cloud size and point count: the TLS deliverable consists of six registered point clouds totalling about 2 billion points, while the PMLS acquisition was delivered as two products: a coloured cloud (about 122 million) and an optimised cloud (about 167 million points). The optimised PMLS product is used for quantitative analyses, while the coloured cloud is retained for visual inspection and figure generation when required.

2.2 Methodology

The proposed methodology was designed to assess the suitability of a PMLS dataset for CH documentation and HBIM-oriented applications, using a previously acquired TLS dataset as geometric reference. The comparison was conceived at two levels: (i) surveys were analysed at dataset level in order to characterize their overall size, point count, and general acquisition properties; (ii) a ROI-based analysis was carried out on selected stable architectural elements, in order to evaluate local geometric agreement, local sampling conditions, and usable completeness with respect to HBIM requirements.

The reference role is assigned to the TLS dataset, which was specifically designed to maximise the completeness and metric reliability for conservation-oriented purposes. The PMLS dataset is instead evaluated in relative terms, i.e., by quantifying its deviation from, and correspondence to, the TLS reference. The analysis was carried out using CloudCompare, version 2.14.

2.2.1 ROI-based comparison strategy: A ROI-based strategy was adopted for different reasons: the two surveys were acquired in different years, and some areas may have been affected by temporary changes unrelated to sensor performance; CH environments include heterogeneous geometries, for which global statistics may mask relevant local behaviours; and, HBIM-oriented applications are usually element-dependent (the adequacy of a point cloud is assessed in relation to the specific architectural component to be represented or analysed. For each selected ROI, the same methodological workflow was applied. After alignment, an equivalent 3D clipping volume was used to extract the corresponding subset from both TLS and PMLS point clouds. In this way, all subsequent metrics were computed on spatially consistent portions of both point clouds.

2.2.2 Local density: In order to characterise the local sampling richness of the point clouds, a density proxy was computed for each ROI. Rather than expressing density only in terms of total point count, which is strongly influenced by the ROI size, a local neighbourhood-based descriptor was adopted. In CloudCompare, this was implemented through the computation of the number of neighbours within a fixed spherical radius (r), stored as a scalar field for each point. A value of r = 1 cm was used as a compromise between two requirements: it is small enough to capture local differences but large enough to provide stable neighbourhood statistics also in sparser point-clouds regions. The resulting scalar field was summarised by means of percentile statistics: P50 was used to represent the typical local sampling condition and P95 was used to describe the upper range of local density values and to capture the variability of point distribution within the ROI. These values are intended as a proxy for the potential level of geometric detail that can be supported by each dataset and are therefore mainly interpreted with respect to LoD-related requirements.

2.2.3 Coverage ratio: In addition to local density, the methodology evaluates the extent to which the PMLS dataset effectively represents the TLS reference surface. For this purpose, a coverage ratio was defined. This is not intended as an absolute completeness metric of a single point cloud, but it is defined as the proportion of TLS reference points within a ROI that find a corresponding PMLS point within a predefined distance threshold. Operationally, cloud-to-cloud distances were computed from the TLS ROI to the corresponding PMLS ROI, thus obtaining a distance scalar field on the TLS points. The coverage ratio at threshold t is defined as:

$$CR_t = \frac{N_{TLS \rightarrow PMLS}(d \leq t)}{N_{TLS}} \times 100, \quad (1)$$

where N_{TLS} is the total number of TLS reference points within the ROI; $N_{TLS \rightarrow PMLS}(d \leq t)$ is the number of TLS points whose cloud-to-cloud distance to the PMLS dataset is smaller than or equal to the adopted threshold t.

To make the metric HBIM-oriented, three thresholds were adopted, each associated with a different target representation scale. These thresholds were derived from the Graphic Error–Tolerance framework: the Graphic Error represents the smallest detail representable at a given scale, while the modelling tolerance is assumed as two to three times the Graphic Error. Accordingly, the following operational thresholds were adopted: t = 5 cm for 1:100 scale; t = 2.5 cm for 1:50 scale; and, t = 1 cm for 1:20 scale. These values correspond to the central values of the tolerance ranges associated with each scale. As a consequence, the coverage ratio becomes a scale-dependent indicator of usable completeness: how much of the reference geometry is effectively represented by the PMLS dataset under the geometric constraints of a given HBIM representation level.

2.2.4 Geometric agreement: The geometric agreement between TLS and PMLS was quantified through the Multiscale Model-to-Model Cloud Comparison (M3C2) algorithm.

This metric was preferred to a simple point-to-point or cloud-to-cloud distance because it is more suitable for comparing point clouds with different densities and local sampling conditions (Lague et al., 2013), especially on curved or irregular surfaces. M3C2 computes signed distances along local surface normals and is therefore more robust in the presence of non-uniform point distributions (Koçak et al., 2025). In the present workflow, the TLS ROI was used as the reference cloud and as the source of core points, while the PMLS ROI was used as the compared cloud. The output consists of a scalar field of signed distances, from which both global bias and magnitude of geometric deviation can be derived. The signed mean distance was retained to describe possible systematic bias between both datasets. In contrast, percentile statistics were computed on the absolute distances $|d|$, since the magnitude of deviation is the most relevant descriptor for HBIM-oriented geometric adequacy (Fasanella et al., 2026). Percentiles were preferred over simple mean values because they provide a more robust description of distributions: P50 represents the typical geometric deviation; P95 describes the upper range affecting most of the points while limiting the influence of a few extreme outliers; and P99 characterises the extreme tail of the distribution in a conservative way. In the present study, these statistics are interpreted in relation to the LoA expected at different HBIM scales. They provide the geometric deviation values that are then compared against the modelling tolerances associated with the intended representation level.

Taken together, these metrics allow the suitability of TLS, PMLS, or hybrid acquisition strategies to be discussed not only as a function of the architectural element, but also in relation to the intended HBIM representation scale and to the actual acquisition geometry.

2.3 ROI selection and results

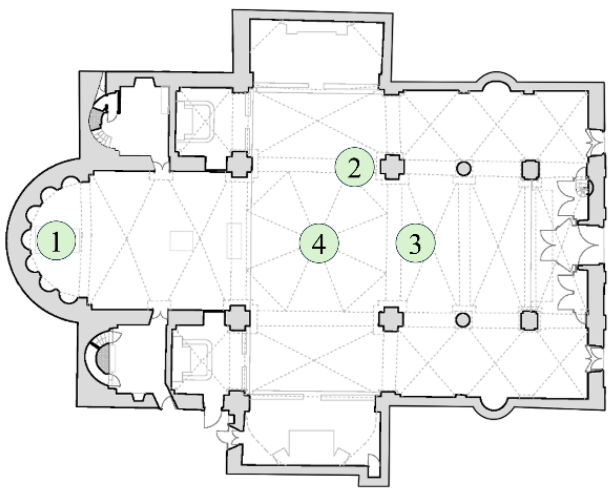

Figure 3. - Keymap of the selected ROIs: (1) the apsis, (2) a pillar, (3) a timber roof truss, and (4) the central dome.

Following the general methodology described above, the quantitative comparison between TLS and PMLS datasets was applied to a set of selected ROIs that satisfy two conditions: (i) they correspond to architectural elements that showed no visible modifications between the two acquisitions, and (ii) they represent different geometric and acquisition conditions, so as to support a more meaningful interpretation of the complementary behaviour of TLS and PMLS.

For each ROI, the same clipping logic and the same set of metrics were applied, thus ensuring methodological consistency across the whole analysis. Based on these criteria, four ROIs were selected (see Fig. 3): the apsis, a pillar, a timber roof truss, and the central dome. Together, these elements represent different combinations of geometry, accessibility, and observation conditions.

2.3.1 The apsis: The apsis (see Fig. 4) represents a geometrically complex but continuous curved macro-surface, thus providing a significant test case for assessing PMLS performance on non-planar CH geometries.

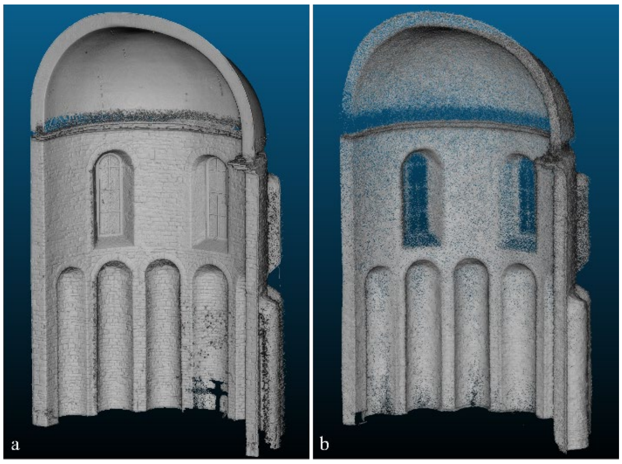

Figure 4. - Comparative view of the apsis ROI extracted from the TLS reference cloud (a) and the PMLS cloud (b).

The floor portion was excluded, since it was affected by temporary objects that differed between the two acquisition times and could bias the comparison. The density analysis shows a marked difference between TLS and PMLS: the TLS cloud returns P50 = 53 and P95 = 88 neighbours, while the PMLS cloud returns P50 = 4 and P95 = 28 neighbours, respectively. This indicates a significantly lower local sampling density for the PMLS dataset on the apsis surface. The coverage ratio confirms that the PMLS dataset remains highly usable at coarser HBIM representation scales but becomes much less complete at stricter thresholds. The values obtained are 98.8% at 1:100, 93.9% at 1:50, and 41.7% at 1:20 scales, respectively. This behaviour suggests that the apsis is strongly affected by the acquisition geometry, particularly by the greater sensor-to-surface distance associated with its upper portions. The M3C2 analysis indicates that the portions effectively measured by the PMLS dataset remain in good geometric agreement with the TLS reference. The signed mean is approximately zero, indicating a negligible global bias, while the absolute-distance statistics produces P50 = 1.3 cm, P95 = 3.0 cm, and P99 = 5.7 cm. Therefore, the apsis appears compatible with 1:100 scale HBIM-oriented modelling or verification, while its suitability decreases significantly when more accurate geometric completeness is required.

https://doi.org/10.5194/isprs-archives-XLIX-B1-2026-151-2026

2.3.2 A pillar: A pillar (see Fig. 5) was selected as a regular vertical structural element. Compared to the apsis, it provides a simpler and more accessible geometry, thus enabling the evaluation of PMLS performance on well-defined architectural components, that are easier to observe from a short distance.

The density analysis highlights a substantial difference between TLS and PMLS datasets also in this case. The TLS cloud returns P50 = 82 and P95 = 128 neighbours, while the PMLS cloud returns P50 = 14 and P95 = 31 neighbours, respectively. However, in contrast to the apsis, this lower density does not correspond to a major loss of usable completeness. Indeed, the coverage ratio remains extremely high across all the adopted thresholds: 99.9% at 1:100, 99.5% at 1:50, and 88.5% at 1:20 scales, respectively. This indicates that the PMLS dataset preserves a very high level of usable completeness on this ROI even under stricter geometric tolerances. The M3C2 analysis confirms this behaviour: the signed mean is -0.2 cm, indicating negligible bias, while the absolute-distance statistics produces P50 = 0.3 cm, P95 = 2.0 cm, and P99 = 6.5 cm. These results indicate very good geometric agreement between both datasets on the pillar ROI. The pillar, therefore, represents a case in which a relatively sparse PMLS cloud may still be fully adequate for HBIM-oriented purposes, provided that the acquisition geometry is favourable.

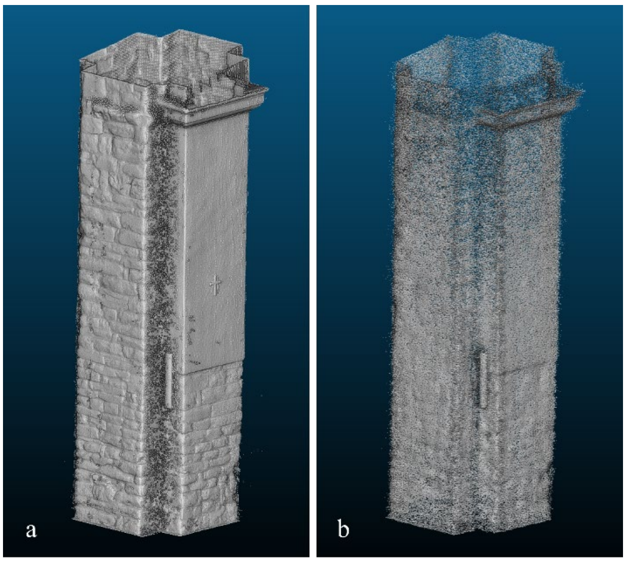

Figure 5. - Comparative view of the pillar ROI extracted from the TLS reference cloud (a) and the PMLS cloud (b).

2.3.3 Timber roof truss: A timber roof truss (see Fig. 6) in the attic was selected as a third ROI to test an articulated structural element characterised by slender linear members, intersections, and local geometric discontinuities.

The density values show that TLS dataset remains locally denser, but the difference with respect to PMLS dataset is less pronounced than in the previous cases. The TLS cloud returns P50 = 39 and P95 = 58 neighbours, while the PMLS cloud returns P50 = 20 and P95 = 55 neighbours, respectively. In particular, the relatively close P95 values suggest that the PMLS dataset preserves a good local sampling richness in the best-observed portions of the truss. This is confirmed by the coverage ratio, which remains very high at all thresholds: 99.9% at 1:100, 99.8% at 1:50, and 92.8% at 1:20 scales, respectively. This result shows that an articulated geometry may still be effectively covered when the acquisition configuration is favourable. In this case, the PMLS survey could be performed directly through the truss structure, while the TLS reference dataset included scans from both sides.

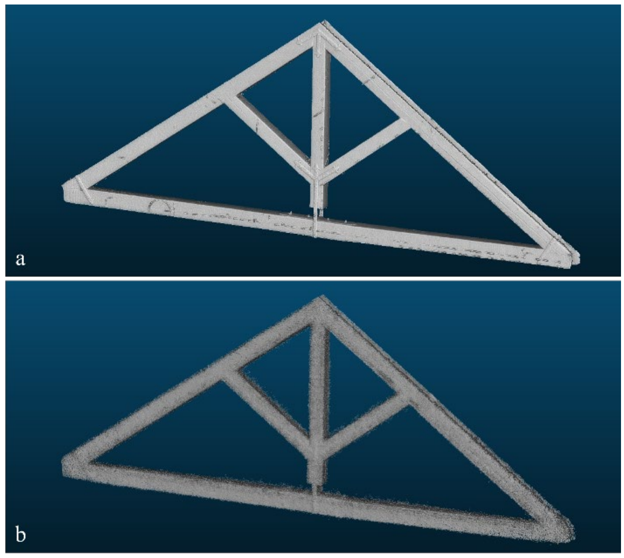

Figure 6. - Comparative view of the truss ROI extracted from the TLS reference cloud (a) and the PMLS cloud (b).

The results based on M3C2 distance are consistent with this interpretation. The signed mean is -3.4 cm, again indicating negligible global bias, while P50 = 0.5 cm, P95 = 4.6 cm, and P99 = 7.8 cm. Therefore, most of the truss ROI remains within the tolerance range associated with 1:100 scale representation, although the upper tail of the distribution reveals local discrepancies likely related to the slender and discontinuous geometry of the members.

2.3.4 Central dome: The central dome (see Fig. 7) was analysed as a high-elevation curved ROI, to verify the influence of the acquisition distance and observation geometry on the results.

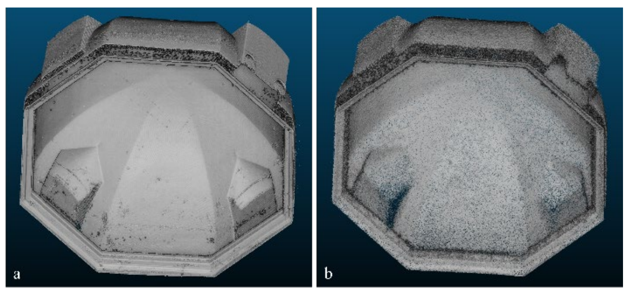

Figure 7. - Comparative view of the dome ROI extracted from the TLS reference cloud (a) and the PMLS cloud (b).

The dome represents a large, curved surface located high above the acquisition path and therefore constitutes an appropriate test case to assess the impact of less favourable observation conditions. The point-density comparison confirms a substantial difference between TLS and PMLS datasets: the TLS cloud returns P50 = 59 and P95 = 85 neighbours, whereas the PMLS cloud returns P50 = 5 and P95 = 12 neighbours, respectively. These values indicate that the dome is one of the sparsest regions in the PMLS dataset among the analysed ROIs. The coverage ratio reveals a clear scale-dependent behaviour. The values obtained are 99.2% at 1:100, 93.2% at 1:50, and only 28.8% at 1:20 scales, respectively. This trend is even more pronounced

than in the apsis and strongly supports the interpretation that the sensor-to-surface distance mainly affects usable completeness under strict modelling tolerances. At the same time, the statistics on M3C2 distance indicate that the portions effectively observed by the PMLS dataset remain geometrically close to the TLS reference: the signed mean is 1.3 cm, while the absolute-distance statistics produce P50 = 1.6 cm, P95 = 2.6 cm, and P99 = 3.8 cm. Therefore, the dome confirms that low density and reduced usable completeness do not necessarily imply poor local geometric agreement. Rather, they indicate that the PMLS dataset accurately represents only part of the reference surface when the acquisition conditions are less favourable.
Table 2 summarises the ROI-based comparison results.

Table 2. - ROI-based comparison results in terms of local density proxy, coverage ratio at scale-dependent thresholds, and M3C2 distance statistics.

	Apsis	Pillar	Truss	Dome
Element type	Curved macro-surface	Vertical structural element	Horizontal structural element	High - elevation curved surface
TLS dens. P50	53	82	39	59
TLS dens. P95	88	128	58	85
PMLS dens. P50	4	14	20	5
PMLS dens. P95	28	31	55	12
Coverage ratio (5 cm) [%]	98.8	99.9	99.9	99.2
Coverage ratio (2.5 cm) [%]	93.9	99.5	99.8	93.2
Coverage ratio (1 cm) [%]	41.7	88.5	92.8	28.8
M3C2 mean signed [cm]	0.0	-0.2	-0.3	1.3
M3C2 P50 |d| [cm]	1.3	0.2	0.5	1.6
M3C2 P95 |d| [cm]	3.0	2.0	4.6	2.6
M3C2 P99 |d| [cm]	5.7	6.5	7.8	3.8

3. Discussion

The obtained results show that no single metric is sufficient, on its own, to describe the suitability of a point cloud for HBIM-oriented applications. Instead, the combined interpretation of local density, coverage ratio, and statistics on M3C2 distance provides a more robust framework for evaluating the complementary behaviour of TLS and PMLS.
Local density describes the richness of point sampling and therefore provides an indirect indication of the level of geometric detail that can potentially be supported during modelling. However, a lower local density does not automatically imply poor usability, as demonstrated by the pillar ROI (Par. 2.3.2), where the PMLS cloud is significantly less dense than the TLS reference but still provides very high coverage ratios and very good geometric agreement.
The coverage ratio proved particularly effective in capturing the extent to which the PMLS dataset remains usable under different HBIM representation scales, describing how much of the reference geometry is represented within a scale-dependent tolerance. For this reason, it is especially informative when comparing ROIs affected by different acquisition distances and visibility conditions.
Finally, M3C2 distance quantifies the local geometric agreement between TLS and PMLS and therefore supports the assessment of LoA-related adequacy. In the present study, the signed mean values remain small for all ROIs, indicating the absence of significant systematic bias after alignment. The percentile-based statistics computed on the absolute distances show that most of the compared points remain within centimetric deviations, although the upper tails of the distributions become more relevant for geometrically articulated or less favourably observed elements.
Taken together, these three metrics show that point-cloud suitability for HBIM cannot be reduced to a single notion of accuracy, thereby confirming the need for a multi-metric evaluation framework.
A first outcome of the study is that the observed differences between ROIs cannot be explained by the geometric complexity alone: the results suggest that acquisition geometry plays a decisive role, in terms of sensor-to-surface distance, accessibility, visibility conditions, and the possibility of acquiring the same element from multiple viewpoints. This interpretation is clearly supported by the selected ROIs: unlike the central dome (Par. 2.3.4), the apsis (Par. 2.3.1) is not uniformly distant from the sensor, as it extends from floor level to the upper vault. Therefore, the observed decrease in coverage at stricter thresholds is interpreted as a progressive effect related to the increasing sensor-to-surface distance towards the upper part of the ROI. In both cases, the PMLS dataset shows very low local density compared with TLS, and the statistics on M3C2 distance remain at centimetric levels, indicating that the portions effectively observed by the PMLS cloud are still geometrically close to the reference. This means that increased distance mainly affects the usable completeness of the dataset rather than the local geometric agreement of the measured surface. The pillar (Par. 2.3.2) shows a different behaviour: despite the much lower PMLS point density, both the coverage ratio and the statistics on M3C2 distance remain very favourable, suggesting that a regular and accessible architectural element can be effectively documented by PMLS even when the local point density is substantially lower than in TLS dataset. The timber roof truss (Par. 2.3.3) is particularly significant because it demonstrates that a geometrically articulated element does not necessarily produce the worst results. Although the truss is more complex than the pillar, the coverage ratio remains very high and the M3C2 values remain acceptable for most of the analysed points. This can be explained by the acquisition configuration: the PMLS survey could be performed directly through the structure, while the TLS reference includes scans from both sides. In this case, the favourable visibility and multi-sided observation compensate for the greater geometric articulation of the element.
The adoption of scale-dependent coverage thresholds provides a useful bridge between point-cloud comparison and HBIM requirements. The results show that the PMLS dataset can be considered highly effective for 1:100 scale-oriented tasks on most of the analysed ROIs, since both coverage and M3C2 values remain compatible with the tolerance associated with that scale.

In several cases, the dataset also remains suitable at 1:50, particularly for regular or well-observed elements. By contrast, the 1:20 threshold highlights a clear reduction in usable completeness for high-elevation curved surfaces, such as the apsis and the dome. This suggests that, while the PMLS dataset may still provide locally accurate data, it is not sufficient to guarantee a complete and reliable representation of these elements at higher-detailed scales. In these conditions, TLS remains preferable, or alternatively, a hybrid strategy should be adopted.
This also means that the same sensor cannot be labelled as universally adequate or inadequate. Its suitability must always be interpreted in relation to: (i) the intended HBIM representation scale; (ii) the type of architectural element; and (iii) the actual acquisition geometry. In this sense, the proposed workflow not only supports a comparison between sensors but also a decision-oriented interpretation of when and how each acquisition strategy should be used.

3.1 Decision matrix

Based on the combined interpretation of the four analysed ROIs in Subsection 3.2, a decision matrix (see Table 3) was derived to relate the choice of sensor to the element type, the expected representation scale, and the acquisition conditions.
In this matrix, ‘suitable’ indicates that the combined behaviour of point density, coverage ratio, and M3C2 distance is consistent with the expected modelling tolerance at the considered scale; ‘conditionally suitable’ indicates that the dataset may support the intended task only for simplified modelling or under favourable acquisition conditions; ‘not sufficient’ indicates that the dataset does not provide adequate usable completeness and/or geometric support for the intended representation scale.
The purpose of the matrix is not to define fixed universal rules, but to provide practical guidance for scan-to-HBIM workflows in CH contexts where time, accessibility, and documentation requirements must be balanced.

Table 3. Decision matrix relating the choice of sensor to the element type, the expected representation scale, and the acquisition conditions: green indicates suitable, yellow indicates conditionally suitable, red indicates not sufficient, and blue highlights hybrid strategies.

Element / condition	1:100 scale	1:50 scale	1:20 scale	Recommended strategy
Curved surfaces with mixed acquisition conditions (e.g., apsis: lower portions closer, upper portions progressively farther)	PMLS suitable	PMLS conditionally suitable	PMLS not sufficient	TLS preferred for upper/high-detail portions; hybrid recommended when rapid full documentation is needed
High-elevation curved surfaces observed at consistently greater distance (e.g., central dome)	PMLS suitable	PMLS conditionally suitable	PMLS not sufficient	TLS preferred; hybrid useful for integrating rapid coverage with accurate reference data
Regular structural elements, accessible and close to the sensor (e.g., pillar)	PMLS suitable	PMLS suitable	PMLS conditionally suitable	PMLS suitable for rapid documentation; TLS when higher detail or stronger geometric control is needed
Articulated structural elements with favourable multi-sided observation (e.g., timber roof truss)	PMLS suitable	PMLS suitable	PMLS suitable / conditionally suitable	PMLS suitable, especially when the structure can be traversed; TLS recommended for detailed joints or conservation-grade analysis
Elements requiring fine geometric detail or strict edge control	PMLS conditionally suitable	PMLS conditionally suitable	PMLS not sufficient	TLS preferred or hybrid
General rapid documentation under time/access constraints	PMLS suitable	PMLS conditionally suitable	PMLS not sufficient	PMLS for fast acquisition; integrate with TLS in critical areas
Mixed scenarios with heterogeneous requirements	Hybrid	Hybrid	Hybrid / TLS	Hybrid strategy recommended

4. Conclusions

This paper compared a static TLS survey and a SLAM-based handheld PMLS survey of San Giacomo Church in Como (Italy), in order to assess the suitability of PMLS data for HBIM-oriented Cultural Heritage documentation. The ROI-based comparison, carried out through local point density, scale-dependent coverage ratio, and statistics on M3C2 distance, showed that PMLS is consistently less dense than TLS, but can still provide satisfactory results where acquisition conditions are favourable.
The results indicate that PMLS is generally suitable for 1:100 scale documentation and, in several cases, also for 1:50 scale applications.
By contrast, stricter requirements reveal clear differences between the analysed elements. The apsis and the central dome show a marked decrease in usable completeness at tighter thresholds, whereas the pillar and the timber roof truss maintain high coverage ratios and acceptable geometric agreement. These findings suggest that the main critical factor is not geometric complexity alone, but the interaction between architectural geometry and acquisition configuration, particularly sensor-to-surface distance, accessibility, and visibility.
The study is limited by the fact that it is based on a single case study and on surveys acquired in different years, which required the selection of stable ROIs and prevented a fully homogeneous whole-dataset comparison.
Future work will extend the analysis to HBIM modelling validation and to the formalisation of LoD/LoA-oriented integration rules for multi-sensor datasets. Overall, the main contribution of the paper lies in demonstrating that TLS and PMLS should be regarded as complementary rather than alternative tools, and in providing a decision-oriented framework

to support more efficient and informed scan-to-HBIM workflows for Cultural Heritage.

Acknowledgements

The research activities carried out in this manuscript are also supported by project TNE23-00012, 'Green & Pink for Sustainable Education' (GPSEducation), funded by Sub-Measure T4 'Transnational Initiatives in Education', Investment 3.4 'University Teaching and Advanced Skills' of the National Recovery and Resilience Plan, Mission 4 'Education and Research', Component 1 'Strengthening the Offering of Education Services: From Nursery Schools to University', for the promotion and implementation of transnational educational initiatives (TNE). The project is funded by the European Union, NextGenerationEU (CUP D74G23000280006).
The authors would like to acknowledge the 'Ente Chiesa Cattedrale di Como', the developers of CloudCompare, and the Stonex Company (specifically, Gianluca Renghini and Giorgio Amendolara) for providing the data acquisition with PMLS.

References

Altuntas, C., Yildiz, F., Scaioni, M., 2016. Laser Scanning and Data Integration for Three-Dimensional Digital Recording of Complex Historical Structures: The Case of Mevlana Museum. *ISPRS International Journal of Geo-Information*, 5(2), paper No. 18, 16 pages, https://doi.org/10.3390/ijgi5020018

Autelitano, K., Bolognini, M., De Angelis, E., Fagiano, L., Scaioni, M., 2023. On the use of drones for vision-based digitalization, diagnostics and energy efficiency assessment of buildings. *Science and Technology for the Built* Environment, 29(10), 985-997, https://doi.org/10.1080/23744731.2023.2261807

Bae, S.J., Park, J., Ham, J., Song, M., Kim, J.Y., 2025. Error Distribution Pattern Analysis of Mobile Laser Scanners for Precise As-Built BIM Generation. *Applied Sciences,* 15(14), paper No. 8076. https://doi.org/10.3390/APP15148076

Catalano, M.,2004. Chiesa di S. Giacomo. Available online at http://www.lombardiabeniculturali.it/architetture/schede/CO181-00005/ (last access on 30/03/2026)

Chen, J., Zhong, J., Ning, Q., Xu, Z., Fukuda, H., 2026. Heritage Conservation and Management of Traditional Anhui Dwellings Using 3D Digitization: A Case Study of the Architectural Heritage Clusters in Huangshan City. *Buildings*, 16(1), paper No. 211. https://doi.org/10.3390/buildings16010211

Del Duca, G., Machado, C., 2023. Assessing the Quality of the Leica BLK2GO Mobile Laser Scanner versus the Focus 3D S120 Static Terrestrial Laser Scanner for a Preliminary Study of Garden Digital Surveying. *Heritage*, *6*(2), 1007–1027. https://doi.org/10.3390/heritage6020057

Della Torre, S., Rajabi, M., 2022. The Restoration of St. James's Church in Como and the Cathedral Museum as Agents for Sustainable Urban Planning Strategies. *Land,* 11(3), paper No. 375. https://doi.org/10.3390/land11030375

Fasanella, Y., Borin, P., Bernardello, R., 2026. Advanced Deviation Analysis Visualization for BIM in Heritage Environment. In: Giordano, A., Russo, M., Spallone, R. (Eds.), *Representation Across Boundaries: New Links with AI, AI-GEN, and XR Tools for Cultural Heritage and Innovative Design* (pp. 925–939). Springer Nature Switzerland. https://doi.org/10.1007/978-3-032-04711-3_53

Garramone, M., Jovanovic, D., Oreni, D., Barazzetti, L., Previtali, M., Roncoroni, F., Mandelli, A., Scaioni, M., 2023. Basilica di San Giacomo in Como (Italy): Drawings and HBIM to Manage Archeological, Conservative and Structural Activities. *International Archives of the Photogrammetry, Remote Sensing and Spatial Information Sciences*, Vol. 48, Part M-2–2023, 653–660. https://doi.org/10.5194/ISPRS-ARCHIVES-XLVIII-M-2-2023-653-2023

Garramone, M., Oreni, D., Scaioni, M., 2023. S. Giacomo Church in Como: Different Modelling Strategies to Create a HBIM for Conservation Activities. In: T. Empler, T., Caldarone, A., Fusinetti, A. (Eds.), *3D Modeling & BIM: Soluzioni per il Cultural Heritage* (pp. 46-57). DEI s.r.l.Tipografia del Genio Civile, Rome. ISBN: 979-12-5505-129-9

Koçak, M.G., Özdaş, N., Kırtıloğlu, O.S., 2025. Visualization of M3C2 Outputs Obtained from an Open Pit Mine Field. *Turkish Journal of Remote Sensing*, 7(2), 218–231. https://doi.org/10.51489/tuzal.1677755

Lague, D., Brodu, N., Leroux, J., 2013. Accurate 3D Comparison of Complex Topography with Terrestrial Laser Scanner: Application to the Rangitikei Canyon (N-Z). *ISPRS Journal of Photogrammetry and Remote Sensing*, 82(2), 10–26. https://doi.org/10.1016/j.isprsjprs.2013.04.009

Liu, J., Azhar, S., Willkens, D., Li, B., 2023. Static Terrestrial Laser Scanning (TLS) for Heritage Building Information Modeling (HBIM): A Systematic Review. *Virtual Worlds*, 2(2), 90–114. https://doi.org/10.3390/virtualworlds2020006

Oreni, D., Jovanovic, D., Barazzetti, L., 2025. Digital Recording of the Domus of Arianna in Pompeii: Toward a HBIM Platform for Site Management. In: Campana, S., Ferdani, D., Graf, H., Guidi, G., Hegarty, Z., Pescarin, S., and Remondino, F. (Eds.), *Digital Heritage* (pp. 1-10). The Eurographics Association, Siena. https://doi.org/10.2312/dh.20253090

Panayiotou, P.N., Kontovourkis, O., 2024. A Holistic Documentation and Analysis of Timber Roof Structures in Heritage Buildings Using Scan to HBIM Approaches. In: *Proc. of the Int. Conf. on Education and Research in Computer Aided Architectural Design in Europe*, Vol. 1, 715–724. https://doi.org/10.52842/conf.ecaade.2024.1.715

Previtali, M., Treccani, D., Garramone, M., Adami, A., Scaioni, M., 2026. Advancements in Portable Mobile Mapping System Point-Cloud Classification: a User-Centric Comparison of Open-Source and Commercial Machine Learning and Deep Learning Solutions. *Applied Geomatics*, 18(1), paper No. 46. https://doi.org/10.1007/s12518-026-00697-z

Rashdi, R., Garrido, I., Balado, J., Del Río-Barral, P., Rodríguez-Somoza, J.L., Martínez-Sánchez, J., 2024. Comparative Evaluation of LiDAR Systems for Transport Infrastructure: Case Studies and Performance Analysis. *European Journal of Remote Sensing*, 57(1), paper No. 19. https://doi.org/10.1080/22797254.2024.2316304

Scaioni, M., Xu, H., Barazzetti, L., Garramone, M., Genzano, N., 2025. Insights of TLS-MLS Current Technology and Foresight for Future Development and Applications. *International Archives of the Photogrammetry, Remote Sensing* *and Spatial Information Sciences*, Vol. XLVIII, Part 5/W3-2025, 109–116. https://doi.org/10.5194/isprs-archives-XLVIII-5-W3-2025-109-2025

Vassena, G.P.M., 2025. Mobile Mapping Approach to Apply Innovative Approaches for Real Estate Asset Management: A Case Study. *Applied Sciences,* 15(14), paper No. 7638. https://doi.org/10.3390/app15147638

Warchoł, A., Karaś, T., & Antoń, M., 2023. Selected Qualitative Aspects of Lidar Point Clouds: GeoSLAM Zeb-Revo and Faro Focus 3D X130. *The International Archives of the Photogrammetry, Remote Sensing and Spatial Information Sciences*, Vol. XLVIII, Part 1/W3-2023, 205–212. https://doi.org/10.5194/isprs-archives-xlviii-1-w3-2023-205-2023